HTML ABSTRACT + LINKS

APPLIED PHYSICS LETTERS **86**, 222104 (2005)

General model and segregation coefficient measurement for ultrashallow doping by excimer laser annealing

Jean-Numa Gillet,[a] Jean-Yves Degorce, and Michel Meunier[b]
Laser Processing Laboratory, Department of Engineering Physics, École Polytechnique de Montréal, C. P. 6079, succ. Centre-ville, Montréal, Québec H3C 3A7, Canada

(Received 19 August 2004; accepted 29 March 2005; published online 24 May 2005)

A general model of ultrashallow doping by excimer laser annealing is derived from only one diffusion-segregation equation. In our model, the relative dopant profile after some laser shots reaches a stationary distribution, which only depends on the segregation and liquid-phase diffusion coefficients of the dopant but not on the laser-process parameters. From this result, a one-point method is proposed to experimentally determine the out-of-equilibrium segregation coefficient k. Only the relative dopant concentration at the material surface has to be measured prior to determine the k value. Experimental dopant profiles are compared to simulations generated with experimental k values. © *2005 American Institute of Physics*. [DOI: 10.1063/1.1927275]

Ultrashallow doping is essential to continue the downscaling for fabrication of the sub-100 nm metal–oxide–semiconductor (MOS) devices.[1,2] For instance, the depth of a PMOS junction needs to be as shallow as 15–25 nm in the 90 nm complementary MOS technology.[3] The formation of ultrashallow junctions also requires rapid and high-temperature annealing to increase dopant electrical activation and remove implantation defects in the silicon. Currently, conventional rapid thermal annealing (RTA) faces the problems of undesired thermal budget, transient-enhanced diffusion, and too low electrical activation, which cannot lead to ideal dopant profiles according to the requirements of the International Technology Roadmap for Semiconductors.[4–6] In order to perform annealing faster and more efficiently, excimer laser annealing (ELA) has recently been proposed by many authors (see Refs. 4–12, for instance) to replace RTA and is now becoming one of the only industrial viable solutions for the formation of ultrashallow doping in ultralarge-scale integrated devices.

Preceding approaches to model dopant diffusion by ELA are derived from the usual Fick equation[7,13,14] or a phase-field method[12] with a heuristic relationship between model equations and the solid-liquid interface velocity (which is usually assumed to be constant during melting and solidification), so that the computed dopant profile depends on the laser-process parameters. To avoid this dependence, we propose a general model for ultrashallow doping by ELA, which is based on only one diffusion-segregation partial differential equation (PDE). The dopant concentration relative to its average value over the maximal melt depth converges, in our model, after some identical laser shots ($N \leqslant 10$) to a stationary profile, which only depends on the segregation and liquid-phase diffusion coefficients of the dopant but not on the laser-process parameters. From this result, we propose a one-point experimental method to determine the out-of-equilibrium segregation coefficient k. Simulations with the k values determined for various dopant types show a very good agreement with experimental profiles obtained after a moderate number of laser shots ($N' \leqslant 100$) by secondary ion mass spectroscopy (SIMS).

If $C(\mathbf{r})$ is the actual concentration of a minority species at the position vector $\mathbf{r}$, its chemical potential μ at $\mathbf{r}$ is given by[15,16]

$$\mu(\mathbf{r}) = k_B T_e \ln[C(\mathbf{r})/C_{\mathrm{ref}}(\mathbf{r})], \tag{1}$$

where k_B is the Boltzmann constant and $C_{\mathrm{ref}}(\mathbf{r})$ is the actual reference concentration, which defines the zero level for μ when the minority species at $\mathbf{r}$ is in thermal equilibrium at the temperature T_e with a Boltzmann distribution.[15] The force $\mathbf{F}$ exerted on the minority species is then derived from $\mathbf{F}(\mathbf{r}) = -\nabla \mu$. Therefore, from a demonstration based on the Einstein relationship and continuity equation (see Ref. 15 for details), we obtain the following PDE for the minority-species concentration $C(\mathbf{r},t)$ at the space-and-time coordinates $(\mathbf{r},t)$:

$$\partial C/\partial t = \nabla \cdot [D(\nabla C - C\mathbf{A})], \tag{2}$$

where $\mathbf{A} = \nabla C_{\mathrm{ref}}/C_{\mathrm{ref}}$ and D is the minority-species diffusion coefficient. The right-hand side of the diffusion-segregation equation in Eq. (2) is made up of two components: The first one, $\nabla \cdot (D \nabla C)$, is the usual Fick diffusion term, while the second one, $-\nabla \cdot (DC\mathbf{A})$, accounts for segregation of the dopant from the solid to the melt, which only appears at the change-of-phase interface where the spatial variation of $\mathbf{A}$ in Eq. (2) takes place. In laser annealing, $C_{\mathrm{ref}}(\mathbf{r})$ has two different values in the solid and liquid zones, which are respectively denoted by K_S and K_L; and the segregation coefficient k is defined as the ratio of the equilibrium dopant concentrations in the solid and melt, so that $k = K_S/K_L \leqslant 1$.[13,14,17,18] From this definition, we obtain $C_{\mathrm{ref}}(\mathbf{r}) = K_L[k + (1-k)\chi(\mathbf{r})]$, where the actual phase distribution $\chi(\mathbf{r})$ is 0 in the solid and 1 in the melt as in phase-field modeling.[12] Therefore, the segregation vector $\mathbf{A}$ in Eq. (2) can be expressed as:

$$\mathbf{A}(\mathbf{r},t,k) = (1-k)\nabla \chi(\mathbf{r},t)/[k + (1-k)\chi(\mathbf{r},t)], \tag{3}$$

and depends on $\mathbf{r}$ and k as well as the time t owing to the moving distribution $\chi(\mathbf{r},t)$, which follows the liquid-solid interface with the time-dependent position vector $\mathbf{r} = \mathbf{r}_i(t)$. In Eq. (3), a discontinuity appears at $\mathbf{r} = \mathbf{r}_i(t)$, because $\nabla \chi(\mathbf{r},t) = \delta[\mathbf{r} - \mathbf{r}_i(t)]$, where $\delta(\mathbf{r})$ is a three-dimensional Dirac function. However, this discontinuity can be avoided by using, as in preceding continuum approaches,[19–22] a continuous transi-

[a]Author to whom correspondence should be addressed; electronic mail: jngillet@videotron.ca
[b]Electronic mail: michel.meunier@polymtl.ca

 © 2005 American Institute of Physics
Downloaded 27 May 2005 to 132.207.1.10. Redistribution subject to AIP license or copyright, see http://apl.aip.org/apl/copyright.jsp

tion of $\chi(\mathbf{r},t)$ from 0 to 1 inside a thin region with a finite thickness (of $\sim$5 nm in our model) around the liquid-solid interface, since this interface can be located by thermal modeling.[23–25] On the other hand, noting that the diffusion coefficient in the liquid phase D_L ($\sim 10^{-4}$ cm^2/s) is higher by several orders of magnitude than that in the solid phase ($\sim 10^{-12}$–10^{-8} cm^2/s),[13] D in Eq. (2) can be approximated by $D(\mathbf{r},t,D_L) \approx D_L \chi(\mathbf{r},t)$ for both liquid and solid subdomains, which leads to an invariant profile $C(\mathbf{r},t)=C_0(\mathbf{r})$ (with C_0 being the initial as-implanted concentration) in the part of the material that is never melted.

Now, we assume an arbitrary laser annealing process with a number of identical laser shots and a melted domain that takes the same maximal volume $\Omega_{\max}$ during each shot. This assumption is reasonable since the needed number N of laser shots to reach the permanent diffusion regime is low enough to avoid a nonreversible modification of the bulk thermal and optical properties. In such a reversible laser process, the dopant concentration solution $C(\mathbf{r},t)$ of Eq. (2) converges after a number of shots $N \leqslant 10$ to a stationary solution $C_\infty(\mathbf{r})$ in the quenched material with the volume $\Omega_{\max}$, which only depends on D_L, k, $\Omega_{\max}$, and the average concentration C_{av} over $\Omega_{\max}$, but not on the laser-process parameters and initial profile $C_0(\mathbf{r})$. Indeed, in Eq. (2), the terms $\nabla \cdot (D \nabla C)$—which tends to make uniform the dopant profile over $\Omega_{\max}$—and $-\nabla \cdot (DC\mathbf{A})$—which tends to push the dopant to the bulk surface—respectively, depend on the parameters D_L and k as well as the distribution $\chi(\mathbf{r},t)$ for both. These are not related to the laser-process parameters in our model, since D_L only depends on the dopant species[13] while k is experimentally measured with a one-point method, as explained in the following, and $\chi(\mathbf{r},t)$ can be assigned, as shown by Eqs. (2) and (3), independently of the moving interface velocity $d\mathbf{r}_i(t)/dt$. Therefore, after a sufficient number of openings and closings of the melted zone, only the same diffusion states $C(\mathbf{r},t)$—the equilibrium solutions of Eq. (2)—can be achieved by the dopant-diffusion process during each laser shot. As a consequence, when the permanent regime has been reached, the unique state $C(\mathbf{r},t) = C_\infty(\mathbf{r})$, which is only related to D_L, k, and $\Omega_{\max}$ as well as C_{av} owing to mass conservation, is sufficient to determine the dopant profile in the quenched material after a laser shot.

Owing to the large dimensions of even few mm^2 of the incident normal beam of the excimer laser,[17] heating can be considered as uniform in ELA, so that the dopant is only redistributed in the x direction, which is perpendicular to the bulk surface.[7,12–14] Therefore, $\mathbf{r}$ and ∇ are replaced by the depth coordinate x with $x=0$ at the material surface and partial derivative $\partial/\partial x$, respectively, in Eqs. (2) and (3); and the dopant concentration solution $C(x,t)$ of Eq. (2) is one-dimensional (1D), assuming a 1D initial as-implanted profile $C_0(x)$. In ELA modeling, the solution $C(x,t)$ of Eq. (2) converges after a number N of identical laser shots to the stationary dopant profile $C_\infty(x)$ in the quenched material with an average concentration C_{av} over the maximal melt depth h. However, after scaling of the space-and-time coordinates in Eq. (2) as $\xi=x/h$ (with $0 \leqslant \xi \leqslant 1$) and $\psi=t/h^2$, respectively, another PDE is obtained in the scaled space time (ξ,ψ) but with the same formulation than that of Eq. (2). Hence, the solution $C'(\xi,\psi)=C[x(\xi),t(\psi)]$ of the other PDE converges again to the same profile $C'_\infty(\xi)=C_\infty[x(\xi)]$, which is now independent of h owing to the scaling. After division by C_{av},

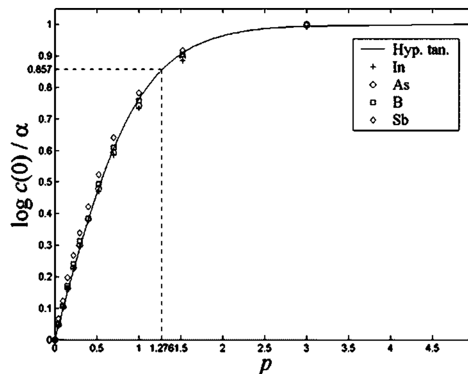

FIG. 1. Curve of $\log c(0)/\alpha$ vs $p=-\log k$ for experimental measurement of k. Computed values of $c(0)$ are shown by $\Diamond$, $\Box$, $\bigcirc$, and $+$ for Sb, B, As, and In, respectively. The full line is the fit $f(p)=\tanh p$ for all dopant species.

we obtain the relative profile $c(\xi)=C'_\infty(\xi)/C_{\mathrm{av}}$, which only depends on the parameters D_L and k. Consequently, $c(\xi)$ is the relative stationary dopant profile of all ELA processes with the same D_L and k.

During ELA, the dopant at the moving interface has insufficient time to segregate with the equilibrium segregation coefficient k_e, so that a $k > k_e$ must be used in Eq. (2).[14,17,18] We propose a one-point experimental method to measure the out-of-equilibrium segregation coefficient k. Our method only requires the experimental measurement of the relative stationary dopant concentration $c(0)$ at the surface $x=0$, assuming that h and C_{av} are known. First, we derived from simulations with Eq. (2) and a finite-element method, an analytical relationship between $c(0)$ and the parameters D_L and k for the dopant in the silicon. We considered the same precomputed thermal process to obtain $\chi(x,t)$ in Eq. (3). After $N \leqslant 10$ laser shots, we obtain relative profiles $c(\xi)$ for four dopant species: Sb, B, As, and In with the values of D_L given in Ref. 13. For each dopant species, we also computed profiles $c(\xi)$ for 13 values of k between 10^{-5} and 1, so that we obtained a database of 52 characteristic profiles $c(\xi)$. From our database, we extracted 52 values of $c(0)$. For each dopant species, we observed the same nonlinear behavior of $\log c(0)$ as a function of the segregation indicator $p=-\log k$. When $p \sim 0$ (i.e., $k \sim 1$), segregation is low and $\log c(0)$ linearly increases with p. However, when $p \sim 1$ (i.e., $k \sim 0.1$), the curve of $\log c(0)$ becomes nonlinear and saturates to a constant plateau when $p \geqslant 3$ (i.e., $k \leqslant 0.001$). By curve fitting with a hyperbolic tangent, we can therefore derive the following approximate analytic relationship between $\log c(0)$ and p:

$$\log c(0) = \alpha(D')\tanh p, \tag{4}$$

where the factor α depends on the dimensionless diffusion coefficient $D'=D_L/D_{\mathrm{ref}}$ with $D_{\mathrm{ref}}=6.9 \times 10^{-4}$ cm^2/s being a reference set to the liquid diffusion coefficient of In. α in Eq. (4) only depends on the dopant species and linearly increases with $\log D'$ for the considered D_L range ($\sim 10^{-4}$ to $\sim 7 \times 10^{-4}$ cm^2/s). Hence, α can be derived from the approximate analytic relationship: $\alpha(D')=b_0+b_1 \log D'$, where $b_0 = 0.840\,201$ and $b_1=0.705\,031$ are fitting constants. Then, by dividing both sides of Eq. (4) by α, one obtains the general behavior of the dopant at $x=0$ after ELA, as shown in Fig. 1, which does not depend on the dopant species. After α is determined, the measurement of the only quantity $c(0)$ en-

Downloaded 27 May 2005 to 132.207.1.10. Redistribution subject to AIP license or copyright, see http://apl.aip.org/apl/copyright.jsp

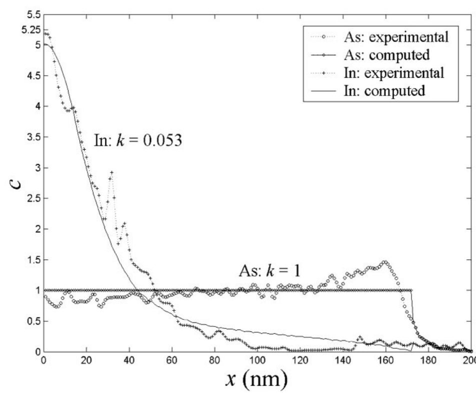

FIG. 2. Experimental vs computed results: Experimental relative profiles are shown by dotted lines marked by + and ○ for In and As, respectively. Numerical profiles, which are computed with experimental k values, are shown by full lines with no mark and ◇ marks for In and As, respectively.

ables us to determine the experimental k value from Eq. (4) or the curve of Fig. 1. Our one-point method avoids the inconvenience of the preceding measurement methods of k, which require one to simulate a large number of dopant profiles associated with several k-values with a full numerical model and then find the best fit with the experimental dopant profile from which the experimental k value is approximately obtained. Consequently, those methods demand the use of sophisticated and computationally expensive software tools for the experimentalist to be capable of measuring k,[7,12–14] in contrast to the one-point method.

Our model has been compared to experimental results. Initial Gaussian profiles of As and In with maximal concentrations of 5×10^{19} cm^{-3} were implanted over a depth of ~100 nm in bulk Si. We performed 100 laser shots on the samples with an excimer laser (wavelength $\lambda=248$ nm, pulse width $\tau=15$ ns, and fluence $\phi=0.6$ J/cm^2) to reach the final dopant concentration profiles. Two experimental relative profiles as obtained by SIMS are shown in Fig. 2 by the dotted curves marked by circles for As and crosses for In. The interface between the transparent cap oxide and the bulk Si is defined at $x=0$. Figure 2 shows that no segregation appears for As, which is approximately redistributed in a uniform (or boxlike) profile over $h=172$ nm, while a strong segregation is present for In, which shows a much shallower profile with a characteristic width of ~25 nm. Experiments performed on In are motivated by the fact that it has recently attracted increasing interest to replace B as a p-type dopant in the sub-100 nm CMOS technologies owing to its heavy mass.[26,27] Moreover ELA is well adapted to In doping, because high solubility and electrical activation of In can be obtained by ELA, but not by RTA.[14] From Fig. 2, we find in our samples $c(0)=1$ and $c(0)=5.25$ for As and In at $x=0$, respectively. Then, with our one-point method, we obtain $k_{As}=1$ (i.e., $p=0$) and $k_{In}=0.053$ (i.e., $p=1.276$) in the As- and In-doped samples, respectively. As expected, these k values are several orders of magnitude higher than those at equilibrium of 0.11 and 4×10^{-4} for As and In, respectively.[17] To validate our one-point method, we computed from Eq. (2) the relative stationary profiles $c(x/h)$ for As and In with the experimental k values. These profiles are rescaled between $x=0$ and $x=h$, and denoted by full lines with no mark for In and diamonds for As. As shown in Fig. 2, both computed profiles fit very well with the experimental ones. In addition, by linear interpolation with a first-order Taylor development, we can obtain with a good approximation from our database a full numerical profile of a dopant related to an arbitrary k value. Therefore, we can also reconstitute with rapidity the numerical profile related to a measured k value without further numerical simulation.

In summary, a general diffusion-segregation model was derived from only one PDE and was applied to ultrashallow doping by ELA. The relative stationary dopant concentration, which only depends on D_L and k in our model, is obtained after some laser shots. From this result, we proposed a one-point method for the experimental determination of the out-of-equilibrium k value, which requires only the prior measurement of $c(0)$ and knowledge of h and C_{av}. Experimental profiles fit very well with simulations obtained with experimental k values.

The authors acknowledge the financial contribution of the Natural Science and Engineering Research Council (NSERC) of Canada.

[1]S.-D. Kim, C.-M. Park, and J. C. S. Woo, IEEE Trans. Electron Devices **49**, 467 (2002).
[2]M. T. Bohr, IEEE Trans. Nanotechnol. **1**, 56 (2002).
[3]R. Duffy, V. C. Venezia, A. Heringa, T. W. T. Hüsken, M. J. P. Hopstaken, N. E. B. Cowern, P. B. Griffin, and C. C. Wang, Appl. Phys. Lett. **82**, 3647 (2003).
[4]C. H. Poon, L. S. Tan, B. J. Cho, A. See, and M. Bhat, J. Electrochem. Soc. **151**, G80 (2004).
[5]K. S. Jones, H. Banisaukas, and J. Glassberg, Appl. Phys. Lett. **75**, 3659 (1999).
[6]B. Yu, Y. Wang, H. Wang, Q. Xiang, C. Riccobene, S. Talwar, and M.-R. Lin, Tech. Dig. - Int. Electron Devices Meet. **1999**, 509.
[7]S. Whelan, A. La Magna, V. Privitera, G. Mannino, M. Italia, and C. Bongiorno, Phys. Rev. B **67**, 075201 (2003).
[8]S. Whelan, V. Privitera, M. Italia, G. Mannino, A. La Magna, C. Bongiorno, C. Spinella, G. Fortunato, L. Mariucci, M. Stanizzi, and A. Mittiga, J. Vac. Sci. Technol. B **20**, 644 (2002).
[9]C. H. Poon, B. J. Cho, Y. F. Lu, M. Bhat, and A. See, J. Vac. Sci. Technol. B **21**, 706 (2003).
[10]S.-D. Kim, C.-M. Park, and J. C. S. Woo, IEEE Trans. Electron Devices **49**, 1748 (2002).
[11]V. Privitera, C. Spinella, G. Fortunato, and L. Mariucci, Appl. Phys. Lett. **77**, 552 (2000).
[12]A. La Magna, P. Alippi, V. Priviterra, G. Fortunato, M. Camalleri, and B. Svensson, J. Appl. Phys. **95**, 4806 (2004).
[13]R. F. Wood, J. R. Kirkpatrick, and G. E. Giles, Phys. Rev. B **23**, 5555 (1981).
[14]C. W. White, S. R. Wilson, B. R. Appelton, and F. W. Young Jr., J. Appl. Phys. **51**, 738 (1980).
[15]H.-M. You, U. Gösele, and T. Y. Tan, J. Appl. Phys. **74**, 2461 (1993).
[16]M. Bailyn, *Survey of Thermodynamics* (AIP, Woodbury, NY, 1994).
[17]D. P. Brunco, M. O. Thompson, D. E. Hoglund, M. J. Aziz, and H.-J. Gossmann, J. Appl. Phys. **78**, 1575 (1995).
[18]R. Reitano, P. M. Smith, and M. Aziz, J. Appl. Phys. **78**, 1518 (1994).
[19]J. A. Kittl, P. G. Sanders, M. J. Aziz, D. P. Brunco, and M. O. Thompson, Acta Mater. **48**, 4797 (2000).
[20]M. Hillert and B. Sundman, Acta Metall. **25**, 11 (1977).
[21]M. Hillert and B. Sundman, Acta Metall. **24**, 731 (1976).
[22]J. W. Cahn, S. R. Coriell, and W. J. Boettinger, in *Laser and Electron Beam Processing of Materials*, edited by C. W. White and P. S. Peercy (Academic, New York, 1980), p. 89.
[23]J.-Y. Degorce, J.-N. Gillet, F. Magny, and M. Meunier, J. Appl. Phys. **97**, 033520 (2005).
[24]H. Kisdarjono, A. T. Voustas, and R. Solanki, J. Appl. Phys. **94**, 4374 (2003).
[25]R. Cerny, V. Chab, and P. Prikryl, Comput. Mater. Sci. **8**, 228 (1997).
[26]S. Scalese, M. Italia, A. La Magna, V. Privitera, M. Bersani, D. Giubertoni, M. Barozzi, S. Solmi, and P. Pichler, J. Appl. Phys. **93**, 9773 (2003).
[27]S. Solmi, A. Parisini, M. Bernasi, D. Giubertoni, V. Soncini, G. Carnevale, A. Benvenuti, and A. Marmiroli, J. Appl. Phys. **92**, 1361 (2002).

Downloaded 27 May 2005 to 132.207.1.10. Redistribution subject to AIP license or copyright, see http://apl.aip.org/apl/copyright.jsp